Sensors and Actuators B 223 (2016) 217–225

Contents lists available at ScienceDirect

Sensors and Actuators B: Chemical

journal homepage: www.elsevier.com/locate/snb

Numerical modeling and experimental validation of a universal secondary electrospray ionization source for mass spectrometric gas analysis in real-time

César Barrios-Collado[a,b,c], Guillermo Vidal-de-Miguel[b,c,*,1], Pablo Martinez-Lozano Sinues[c,*,1]

[a] Department of Energy Engineering and Fluid Dynamics, University of Valladolid, Spain
[b] SEADM S.L., Spain
[c] Department of Chemistry and Applied Biosciences, ETH Zurich, Zurich, Switzerland

ARTICLE INFO

Article history:
Received 30 June 2015
Received in revised form 3 September 2015
Accepted 14 September 2015
Available online 16 September 2015

Keywords:
Vapors
Volatile organic compounds
Real-time detection
Mass spectrometry
Gas analysis

ABSTRACT

The process by which ambient vapors are ionized upon interaction with electrosprays is not fully understood, compromising its optimization and widespread use. In this work we evaluated the different scales associated with the processes involved in secondary electrospray ionization (SESI), and developed a new numerical method that merges the analytical solution that describes the angle of aperture and the current of an ideal electrospray, with a finite element method that enables the evaluation of complex geometries. The numerical method showed that, despite the low ionization efficiency (i.e. ion concentration/neutral vapor concentration $\sim 10^{-4}$), depletion of neutral vapors plays an important role. We used this method to optimize and design a low flow SESI source, which was coupled with a commercial high resolution/high mass accuracy mass spectrometer. The system was designed to be interfaced with virtually any pre-existing atmospheric pressure ionization mass spectrometer. The experimental validation for the detection of ambient vapors confirmed qualitatively the numerical predictions in terms of ionization efficiency as a function of sample flow rate. As a result of the optimization, this prototype showed a 5-fold sensitivity increase against standard SESI. This novel add-on is meant to upgrade mass spectrometers to analyze trace gases in real time by SESI technique.

1. Introduction

The fact that electrosprays lead to the ionization of gas-phase molecules was noticed independently by Fenn and coworkers [1–5] and Wu, Hill and colleagues, who found that electrosprays were an attractive alternative to other more conventional approaches (e.g. radioactive sources) for the ionization of vapors [6,7]. As a result, this peculiar ionization process has been dubbed secondary electro-spray ionization (SESI) [8–10]. SESI is mainly used to ionize polar compounds leading typically to protonated or deprotonated species, depending on the ionization mode. Other ionization techniques also use an electrospray as a primary source of ions (a more complete review can be found elsewhere [11,12]): desorption electrospray ionization [13], extractive electrospray ionization [14], laser ablation electrospray ionization [15] or fused droplet electrospray ionization [16]. However, the term SESI is here restricted to the ionization of vapors. coupled with atmospheric pressure interface mass spectrometers (API-MS), it has been successfully used detect various types of analytes including explosives [17], chemical warfare agents simulants [18], drugs [19], human metabolites [20–23], food [24,25] and bacterial emissions [26,27].

The mechanism by which electrosprays of pure solvent such as water lead to the ionization of vapors remains to be fully understood [28]. Although the process is thought to be driven by gas-phase ion molecules reactions [29], which takes place at the sub-micrometer scale. As a result, the macroscopic description of the process can be decoupled from the actual charge exchange mechanisms. This assumption led to the development of the first theoretical models that describe the ion concentration distribution: the model described in [30] predicts a uniform Damköhler number p_i (defined as the ratio of the concentration ions generated over the concentration of molecules) in the limit of very low

* Corresponding authors at: ETH-Zurich, Department of Chemistry and Applied Biosciences, ETH Zurich, Laboratory of Organic Chemistry D-CHAB, HCI E 331, CH-8093 Zurich, Switzerland.
E-mail addresses: guillermo.vidal@org.chem.ethz.ch (G. Vidal-de-Miguel), pablo.mlsinues@org.chem.ethz.ch (P. Martinez-Lozano Sinues).
[1] Co-senior authors.

http://dx.doi.org/10.1016/j.snb.2015.09.073

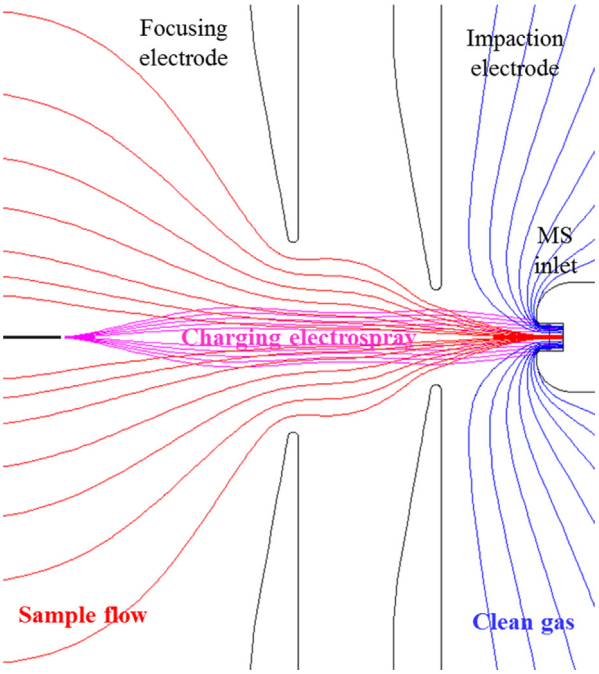

Fig. 1. LFSESI basic architecture. (For interpretation of the references to color in the text, the reader is referred to the web version of this article.)

vapor concentrations, while the model described in [31] provides a more general relation between the concentration of charging ions (i.e. the primary ions produced by the spray) and sample ions (i.e. the ionized vapor molecules). These theories are in accordance with experimental measurements [17]. Based on this qualitative understanding of the concentration of ions within the electrospray plume, the concept of low flow SESI (LFSESI) was developed to minimize the consumption of vapors and to maximize the electrostatic flow of ions [32]. Fig. 1 illustrates the basic architecture of a LFSESI, in which the ionization region is separated from the MS inlet region by means of a plate that prevents the sample vapors (red streamlines) from being diluted by the flow sampled by the MS (blue streamlines). Additionally, this plate produces an intense electric field that creates a narrow ion beam which aims at the API-MS inlet. Compared with conventional SESI sources, which have an "open" configuration, the flow consumed by LFSESI can be highly reduced, concentrating the sample and thus increasing the ionization efficiency as a result. However, This LFSESI was not optimized because no numerical methods were available to solve all the physical problems involved.

A complete SESI description by a numerical model, including electrospray formation, charge transfer reactions and the interaction with the fluid fields is lacking. The first goal of this study was to fill this gap by developing a method to accurately model SESI at the macroscopic scale. This is interesting for two reasons: (i) it can be used to better understand the measured results, by isolating pure mechanistic reactions (the microscopic level) from other macroscopic effects, and to (ii) optimize the design of ion sources. Accordingly, the second goal of the present study was to develop a commercially available and optimized low flow SESI (LFSESI) [18] source. The performance of this new prototype was benchmarked against a state-of-the-art SESI system using drugs as target vapors.

2. Methods

In this section we analyze the physical processes involved in the expansion of an electrospray plume. Subsequently, we describe a new algorithm developed to model SESI. Finally, an optimized prototype was constructed and experimentally validated.

2.1. SESI modeling

2.1.1. Background

Finite element methods (FEM) Multiphysics solvers – such as COMSOL – for partial differential equations (Eulerian approach), allow to combine fluid mechanics, electrophoretic transport of species, chemical reactions, and electrostatic fields (including space charge effects). In view of this, one could think that COMSOL has all the tools required to simulate an expanding electrospray plume. However, the shape of the plume is much defined by the singularity of the tip of the spray, which cannot be addressed numerically. Moreover, the different scales involved in a SESI – the tip of the spray is typically in the sub-micrometer range, and the expanding plume is in the mm range – hinder the Eulerian approach.

For this reason, the numerical analysis of an electrospray expansion typically relies on a Lagrangian formulation, usually combined with droplet evaporation models [33,34]. These methods compute the trajectories of the particles, incorporate the evolution of the droplets to calculate the shape of the plume, and also incorporate Coulomb repulsion between particles to account for space charge effects. These methods provide useful insight on how nano-drops evolve into ions, which is of great use in ESI sources. However, these methods are difficult to couple with FEM solvers, which are better suited to evaluate the most downstream parts of the electrospray plume. This is crucial, since we know that this area plays a key role in SESI mechanism, as suggested by theoretical studies [30,31].

In the present work we addressed this problem by implementing a simple and reasonably accurate numerical model of the electrospray phenomena, which describes electrospray dynamics as a continuum in order to use FEM solver. The main obstacles to achieve this objective are the difference of scales involved and the singularity at the meniscus.

Fortunately, since the typical charging solutions used in SESI are highly conductive, and use simple and small ions (such as chloride, formic acid, or ammonia), the resulting electrosprays are well characterized. The process by which charging ions are produced can be simplified. We used the solution proposed by Fernandez de la Mora [35] to handle the singularity at the apex of the meniscus with analytical expressions. This analytical solution was bridged with a FEM solver to describe the expansion of the plume, which depends on the far-field geometries, voltages, and gas flows.

2.1.2. Development of a numerical method

The mathematical model described by Fernandez de la Mora [35] is based exclusively on electrostatics for the emission of electrified liquid cones which relates the meniscus angle, the plume expansion and the intensity emitted by the electrospray. This model has the following assumptions: (1) the meniscus and the spray form two ideal and infinitely large opposed cones; (2) it ignores the microjet that transitions between the meniscus and the expanding plume, and the droplet formation dynamics; (3) the liquid is infinitely conducting (assumable for conductivities higher than 0.03 S/m); (4) all droplets have the same charge, size and electrical mobility; (5) neglects droplets inertia, the scale of the micro-jet, droplet evaporation, and diffusivity. Thus, although this model is limited to the ideal case of an electrospray plume expanding to infinity (i.e. it does not take into consideration real geometries), it is valid in the proximity of the meniscus tip because its length-scale is far smaller than the meniscus itself. The validity of these assumptions in the near-field (i.e. close to the electrospray tip) in the SESI problem formulation is further discussed in Supporting information.

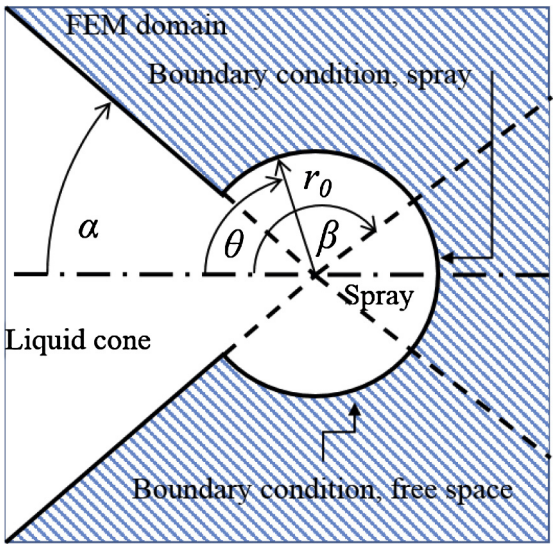

Fig. 2. Electrospray modeling.

2.1.3. The initial expansion of the plume: bridging the singular solution with the FEM model

The singularity region and the far field region can be easily modeled, but the physical processes taking place in the transition region are far more complex. Nevertheless, since all ions and droplets in this region emanate from the singularity region, which is spherically symmetrical, their trajectories are all rectilinear in first approximation. As a result, regardless of the particular evolution of the droplets, the imaginary interface that separates the transition region from the far-field region is a sphere centered in the electrospray tip, and the concentration of charge along this imaginary sphere is given by the concentration in the smaller sphere defined by the imaginary interface between the singularity region and the transition region. Since spherical symmetry is conserved along the transition region, and given that diffusion effects are negligible in this region (due to the high ionic velocities), we can assume that the charge concentration defined by Fernandez de la Mora's model can be directly inputted in the spherical interface between the transition region and the far-field region regardless the droplet particular evolutions along the transition zone. In other words, we can directly link the analytical model with the far-field region through a spherical boundary condition centered at the tip of the electrospray.

Fig. 2 shows a scheme of the domain shape that incorporates a spherical cap centered about the electrospray tip, as well as a conical meniscus. The radius r_0 of the cap was half the capillary radius, and the electric potential and the ion concentration boundary conditions on the cap were defined in accordance with the analytical solution for free space or spray at radial coordinate r_0, given by [35]. The meniscus and spray angles α and β were interpolated from tabulated data (Table S1, reproduced from [35]), as a function of: (i) $G(\alpha) = I/(2\pi\gamma Z)$; ii) the spray current (I); (iii) the liquid surface tension (γ) and (iv) the ion mobility (Z). The electric potential (V) and the charge concentration (ne^-) followed Eqs. (1) and (2), respectively:

$$V = \begin{cases} V_0 - \sqrt{\dfrac{2I\ \sin 2\alpha r_0}{3\pi\varepsilon_0(1+\cos\beta)Z}}\dfrac{P(\alpha)Q(\theta)-Q(\alpha)P(\theta)}{0.63662}, & \alpha \le \theta \le \beta \\ V_0 - \sqrt{\dfrac{4Ir_0}{3\pi\varepsilon_0(1+\cos\beta)Z'}}, & \beta \le \theta \le \pi \end{cases} \quad (1)$$

$$ne^- = \begin{cases} 0, & \alpha \le \theta < \beta \\ \sqrt{\dfrac{3\varepsilon_0 I}{4\pi(1+\cos\beta)Z{r_0}^3}}, & \beta \le \theta \le \pi \end{cases} \quad (2)$$

where V_0, θ, $P(\theta)$ and $Q(\theta)$ are the electrospray voltage, the angular coordinate and two independent Legendre functions of degree 1/2 and order 0.

This model allowed us to calculate with reasonable accuracy the spatial concentration of electrosprayed ions by knowing the properties of the liquid (surface tension and conductivity) and the operating conditions (voltages and electrospray intensity), with a purely electrostatic model.

2.1.4. Reactive flow

Near the electrospray tip the concentration of charging ions is very high, and due Coulomb forces, the plume expands abruptly so the charging ions get diluted into the sample flow. Theoretical models [30,31] consider two ionization mechanisms: (i) ionization of molecules by ions via chemical ionization; and (ii) ionization of vapors by droplets, where the neutral vapors are dissolved into the droplets and get ionized. Experimental studies [29] suggest that the ion–molecule reaction is the dominant mechanism in SESI. Hence, ionization reactions were considered only in the far-field region, where droplets are already evaporated.

We based the numerical model of the SESI reaction kinetics on [30,31]. The evolution of the concentrations was modeled according to the ordinary differential equations system given by Eq. (3) which includes the reaction kinetics as well as the convective and diffusive transport. Note that the latter was conveniently neglected in the electrospray model in order to adapt the analytical solution, but it was considered in the rest of the domain,

$$\begin{cases} \dfrac{dc_c}{dt} = -kc_c c_v - \nabla\cdot(c_c(Z_c\vec{E}+\vec{v}_f)) + \dfrac{Z_c k_B T}{e^-}\nabla^2 c_c \\ \dfrac{dc_v}{dt} = -kc_c c_v - \nabla\cdot(c_v\vec{v}_f) + D\nabla^2 c_v \\ \dfrac{dc_i}{dt} = kc_c c_v - \nabla\cdot(c_c(Z_i\vec{E}+\vec{v}_f)) + \dfrac{Z_i k_B T}{e^-}\nabla^2 c_i \end{cases} \quad (3)$$

where c_c, Z_c, c_v, c_i and Z_i are the concentrations and mobilities of charging ions, neutral vapors and ionized vapors respectively; E, v_f, k_B, T and D are the electric field, the fluid velocity, the Boltzmann's constant, the absolute temperature and the neutral vapor diffusivity (diffusivities of charging ions and ionized vapors are represented by the Einstein relation, and the diffusivity of neutral vapors D was estimated as being equal to their corresponding ions) respectively; and k is the reaction kinetic constant. SESI process is thought to occur by, first ejection of hydronium clusters (i.e. $(H_2O)_nH^+$) from charged electrospray droplets, which ultimately lead to gas-phase proton transfer reaction to neutral vapors [29]. Collisional rate constants for proton transfer reaction can be estimated using the Langevin's equation [36] or more sophisticated models to account for additional effects such us polarizability [37–39]. Thus, typical values for ion-molecule reaction rate constants for proton transfer reactions between H_3O^+ and volatile organic compounds range between 1×10^{-9} and 5×10^{-9} cm^3 s^{-1} [40]. For such product ions ($m/z \sim 200$ Da), typical electrical mobilities lie in the range $Z_i \sim 1$–2 cm^2/V/s. These k and Z_i values can finally be used to bracket the dimensionless Damköhler number (p_i) as defined in [30].

$$p_i = \left(\frac{c_i}{c_v}\right) = \frac{k\varepsilon_0}{qZ_i} \quad (4)$$

where ε_0 is the vacuum permittivity and q the ionized vapor charge. Hence, typical Damköhler numbers range between 10^{-3} and 10^{-4}.

2.1.5. Fluid dynamics

The maximum sample flows considered in the LFSESI are in the order of 1 L/min (1.67×10^{-5} m^3/s). For this flow, and for the typical orifice sizes used (i.e. 2 mm for the impact orifice), the Reynolds number is ~709, which is well below the critical *Re* (~2000). Accordingly, a laminar flow model was used. The domain included a sample inlet, an outflow to the MS capillary inlet whose flow rate was set at 1.6 L/min (2.67×10^{-5} m^3/s), which is characteristic of Thermo-Fisher instruments at atmospheric pressure conditions.

2.1.6. Numerical method implementation

The whole numerical model was implemented in commercial FEM software COMSOL Multiphysics. To improve computational resources, the model was built considering axial symmetry. We took advantage of an iterative mesh refinement algorithm available in COMSOL. Starting from a coarse mesh (3734 elements), the algorithm re-meshed those areas affected by high gradients, such as the areas close to the electrospray tip (high electric fields), the MS inlet (high fluid velocity gradients), and the boundary layers that separate the plumes from the clean regions. The parameters investigated were (i) sample flow rate; (ii) electrospray current; (iii) axial position of the emitter with respect to the focusing and impaction electrodes and MS inlet; and (iv) orifice sizes. Each simulation took around 2 min to be computed.

2.2. Experimental validation

Based on our numerical method, we built an optimized geometry, and benchmarked its performance against a "standard" SESI source. By "standard" we mean a nano-spray emitter enclosed in a cylindrical chamber facing the MS orifice, but not featuring any plate decoupling the ionization region from the curtain gas. Such chambers have been used in multiple studies.

To validate the SESI sources we delivered precise amounts of target vapor species and measured the resulting mass spectral signal intensity. The experimental set-up is described in detail elsewhere [17,18,41]. Briefly, the vapor generator was a secondary electrospray enclosed in a heated chamber. Electrosprayed solutions of the species of interest dissolved in H_2O were mixed with a controlled flow of clean nitrogen. In this study we used as sample species diethylamine (DEA) and the drugs melatonin, propofol, paracetamol, pentobarbital and midazolam. Under the assumption of Poiseuille flow $Q = \pi R^4 \Delta P/(8\mu L)$, where Q is the flow rate R is the electrospray capillary inner radius, ΔP the pressure drop, μ the liquid dynamic viscosity and L the capillary length), the flow rate of the sample species could be calculated, and thus the gas phase concentration of the sample flow. Typically, to obtain low parts-per-trillion (ppt) concentrations in the gas-phase, we used liquid samples at concentrations in the ng/mL range, infused at ~1 μL/min and diluted in nitrogen at flow rates ranging 0.2–1.6 L/min. The vapor generator and the clean nitrogen line were heated up to 190 °C, and the temperature was controlled by a proportional-integral-derivative controller. In these experiments the temperature of the ionization source was set to 85 °C (PID controlled), limited by the charging agent (H_2O–formic acid 0.1%) boiling point. MS sweep flow was set to 4 (arbitrary units) and the inlet capillary temperature was set to 200 °C. Voltages, mechanical alignment and electrospray tip axial position were optimized prior the experiments.

The LFSESI used in this study was a novel design developed at the ETH-Zurich in collaboration with SEADM S.L., based on the numerical studies described in this work. This device consists basically on a heated asymmetric LFSESI chamber which is coupled to the MS atmospheric pressure interface. A 2-axis micrometric positioning system provides fine mechanical alignment between the LFSESI and the MS inlet capillary. Also, the axial position of the electrospray tip can be optimized manually. The core of the ionizer was housed in an interface compatible with Thermo-Fisher mass spectrometers. In this case, we interfaced the ionizer to a Thermo-Fisher LTQ Orbitrap. Similarly, different housing for other vendors such as Sciex are available. Fig. 3a shows a picture of the mass spectrometer with its standard ESI source (meant for liquid

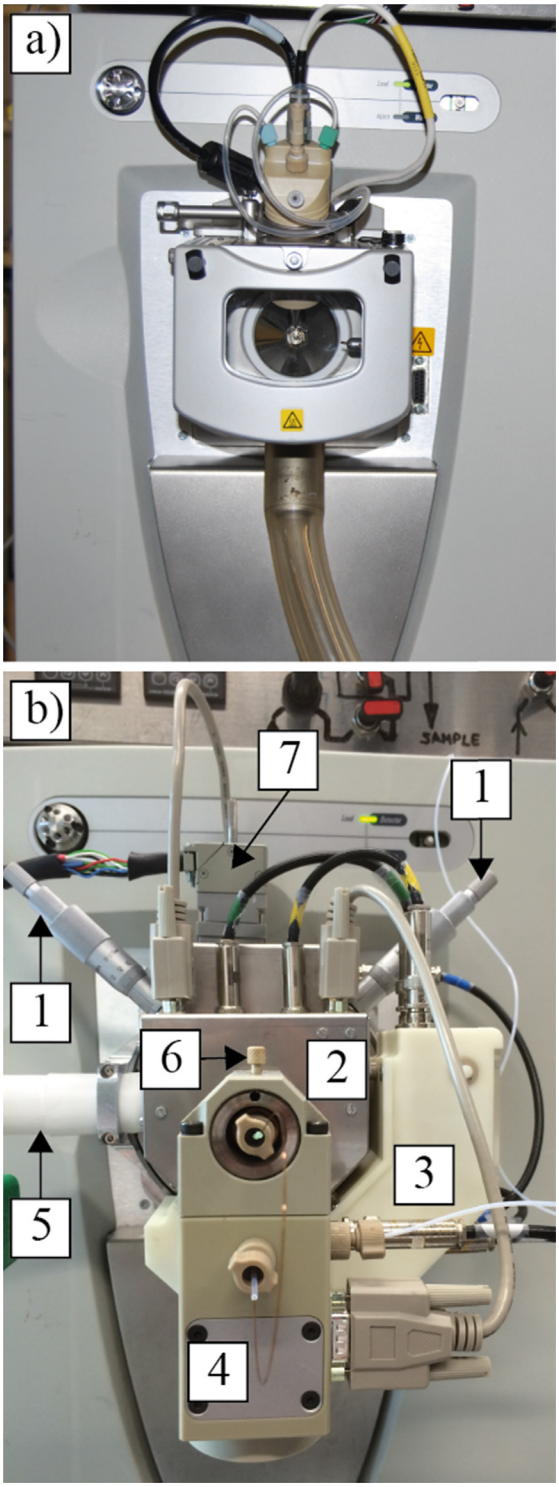

Fig. 3. Orbitrap mass spectrometer with: (a) standard Thermo-Fisher ESI source; (b) LFSESI: (1) Mechanical alignment; (2) thermal insulation surrounding the core; (3) high voltage electronics module; (4) electrospray vial holder; (5) transfer line; (6) electrospray positioning; (7) temperature control connection for core and transfer line.

samples only). Fig. 3b shows a picture of the vapor ionizer interfaced with the Orbitrap. The exchange between both ion sources takes less than 5 min and requires no modifications of the MS.

3. Results and discussion

3.1. Electrospray model validation

In order to test the new numerical model for the electrospray, we simulated the experiment in described in [35], where a capillary at 3715 V sprays against a grounded plate at 7 mm form the tip a solution of H_2SO_4 (5%) in 1-octanol. Fig. 4 shows a comparison between the photographs from the original experiment (reproduced with permission) and the simulated ion concentration contours. The simulations recreate the plume expansion close to the experimental results. The menisci angles were found to be slightly wider in the simulations. This overestimation may be the result of no considering the feedback electrostatic effect of the plume on the meniscus; however this effect is also present in the analytical model. So, we concluded that the approximation was reasonably good to be included in the general SESI model.

3.2. Fluid dynamics optimization

In order to study the effect of the LFSESI impaction plate design parameters, we studied the flow patterns in the vicinity of the sampling capillary of a Thermo Fisher Scientific mass spectrometer. The objective of this study was to optimize the impaction plate orifice diameter (d) and distance (l) from the MS sampling capillary. The optimal flow configuration should separate efficiently the ionization region from the MS clean gas region to avoid dilution of vapors and prevent turbulence, hence maximizing the ions transmitted to the MS. We found two possible flow configurations. When l and d are in the same order, the sample flow produces a jet that travels smoothly toward the MS inlet. However, when $l \ll d$, recirculation cells are formed, increasing as a result undesirable memory effects. Fig. S1 shows the flow fields for both configurations.

3.3. Electrostatic optimization

Fig. 5a–c shows the surface plots of the concentrations of charging ions (c_c), neutral vapors (c_v), and ionized vapor (c_i) for a sample flow of 0.05 L/min (8.33×10^{-7} m^3/s) and an electrospray tip positioned at 5 mm from the focusing electrode. Fig. 5d–f show the corresponding concentration profiles of charging ions, neutral vapors and ionized vapors along the radial coordinate. The simulations considered a realistic scenario where the charging ions (H_3O^+) were produced from an electrospray of water (0.1% formic acid) and 8.5 ppt of DEA as neutral vapors.

As expected, close to the electrospray tip the concentration of charging ions is very high, and it decreases quickly with the distance to the electrospray tip (noticeable in the logarithmic scale). The ionized vapors cloud has the same shape as the electrospray plume, but the concentration is at least seven orders of magnitude lower than the charging ion concentration, supporting the hypothesis of theoretical models that electric field distortions due to space charge are essentially caused only by charging ions. As expected from the high *Pe* numbers, diffusion effects are noticeable only at the borders of both charging ion and ionized vapor clouds.

We found that the electrospray cloud does not vary at different neutral vapors concentration, which validates the common accepted assumption of negligible depletion of charging ions. However, in contrast to the assumptions made by theoretical models, the concentration of neutral vapors is not constant. We found a significant decrease of neutral vapor concentration along the electrospray plume (Fig. 5b and e).

Due to the low Damköhler number ($p_i \sim 10^{-3}$–10^{-4}), it is commonly accepted that the concentration of neutral vapors should be constant. However, these detailed simulations suggest that electric fields drive ionized vapors outside the ionization region too fast to be replaced by fresh neutral molecules. This effect causes a depletion of neutral molecules in the core of the electrospray plume and also is responsible of making the highest concentration of ionized vapors on the periphery of the plume, where fresh neutral molecules and charging ions meet easier. Unfortunately, these ions are not transmitted to the MS as their trajectories die in the LFSESI electrodes, so the ionic flow produced by the ionizer comes from the depleted region.

Moreover, we found that these spatial non-uniformities of neutral and ionized vapors concentrations become more important as the sample flow is reduced, counteracting as a result the beneficial concentration enhancement associated with low sample flows. This raises some questions about where the optimal sampling flow rate is. This important parameter was assessed by evaluating ionization efficiency. The theoretical ionization efficiency is given by $\eta_i = p_i q_{ms}/q_s$, where η_i, p_i, q_{ms} and q_s are the ideal ionization efficiency, the Damköhler number, the flow entering by the MS and the sample flow, respectively. The simulated ionization efficiency was calculated as $\eta = c_i q_{ms}/(c_v q_s)$ where η_i, c_i, and c_v are the ionization efficiency, the concentration of ionized vapors at the MS inlet and

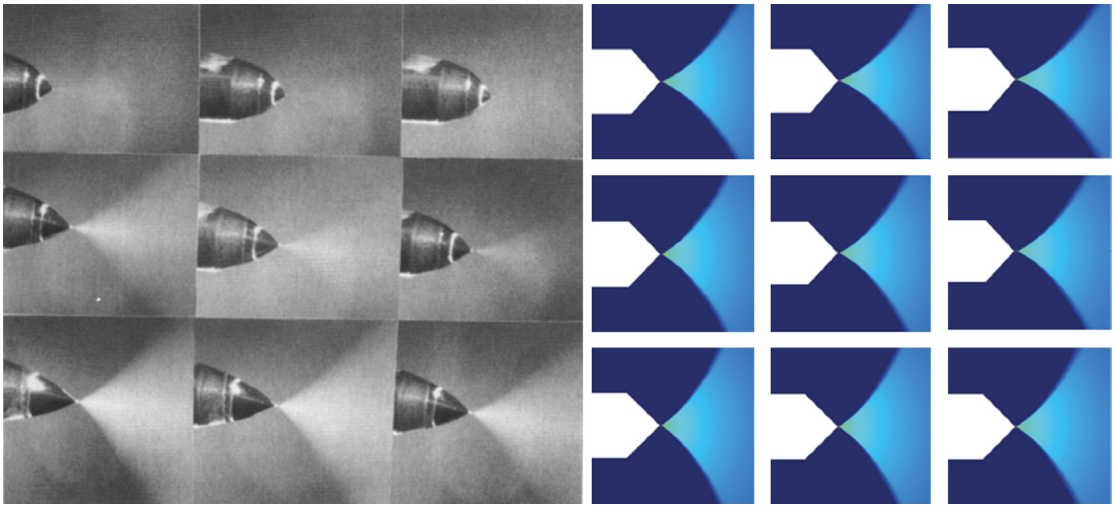

Fig. 4. Left: experimental electroprays [35] (reprinted with permission); right: simulated electrosprays.

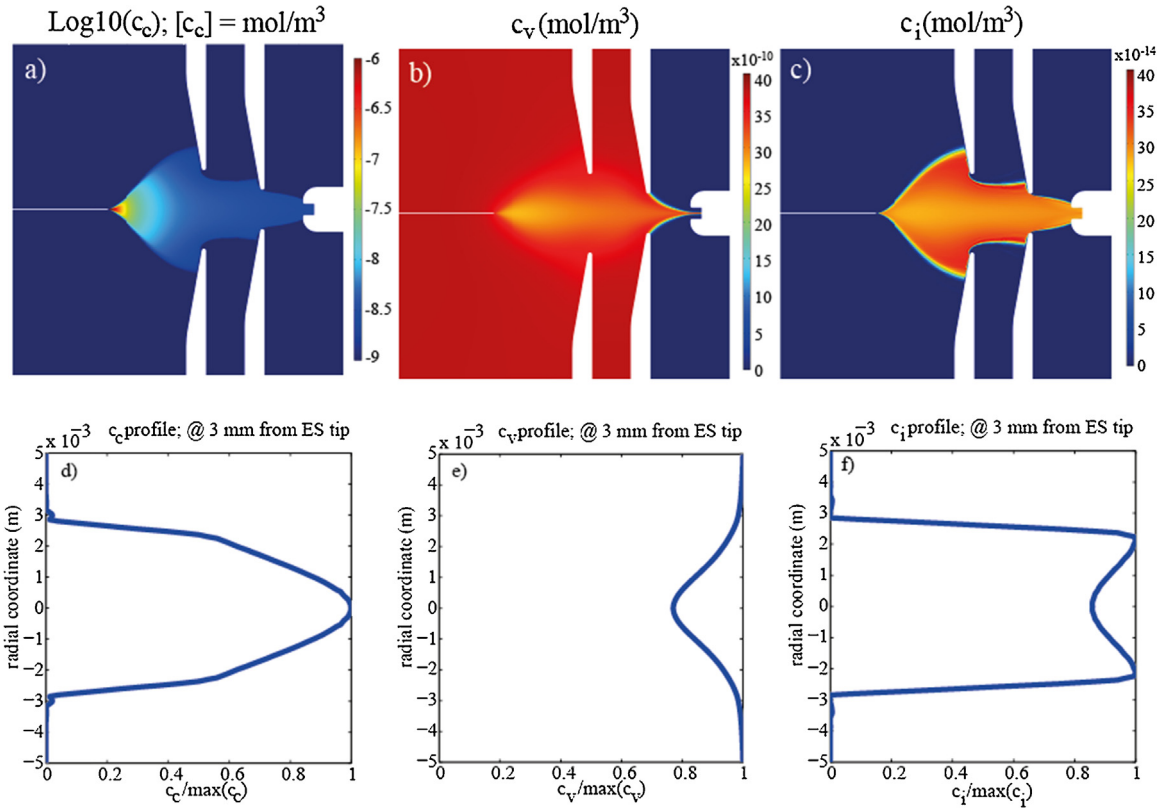

Fig. 5. Contour plots and radial profiles at 3 mm from the electrospray tip of the concentration of involved species: (a, d) charging ions; (b, e) neutral vapors; (c, f) ionized vapors; q_s = 0.05 lpm; q_{ms} = 1.6 lpm; Y = 5 mm; electrospray of H_2O-HCOOH (0.1%); c_v = 8.5 ppt of DEA.

the concentration of neutral vapors at the sample flow inlet respectively. In other words, the ionization efficiency was computed as the ratio of the flow of ions that entered the capillary of the MS over the flow of neutral vapors that entered the ionizer.

Fig. 6a shows a comparison of ideal and simulated ionization efficiencies for four different electrospray currents (20, 50, 100 and 200 nA) as a function of sampling flow rate. The MS sampling flow rate was set to 1.6 L/min, which is the actual flow ingested by the Orbitrap MS used in our experimental validation. One can observe that at high sample flows, the simulated ionization efficiency follows the theoretical one. As expected, ionization efficiency increases as the sample flow is reduced because the target vapors are concentrated. At flow rates above 0.2 L/min, the transport of neutral vapors to the ionization region is efficient, and thus the depletion is not noticeable. However, at flows below 0.2 L/min, although ionization efficiency still increases, its rate is clearly lower than the theoretical one due to the depletion of vapors. This effect becomes more dramatic with increasing electrospray currents. This can be explained because at increasing electrospray currents, space charge effects become more dominant, widening the plume as a result. The net result is that the vapor depletion region becomes larger.

In an attempt to further understand this phenomenon, we extended the simulations. Fig. 6b shows a dimensionless representation of the ratio between simulated and ideal efficiencies vs. sample flow rate over MS flow rate (i.e. 1.6 L/min). The figure shows the results for the combination of three different paired kI values, where k is the reaction kinetic constant and I the electrospray intensity. This representation was chosen because kI is proportional to the term kc_cc_v in Eq. (3), which is responsible for vapor depletion. We scanned three kI groups (2×10^{-7}, 2×10^{-8} and 2×10^{-9} nA cm^3 s^{-1}) across four realistic intensity values (20, 50, 100 and 200 nA). Thus, 12 values for the collisional rate constant (k) were scanned ranging from 1×10^{-11} to 1×10^{-8} cm^3 s^{-1}. As expected by Eq. (3), we observed three clusters for each kI group and a closer ideal behavior for smallest kI product (i.e. 2×10^{-9} nA cm^3 s^{-1}). These results confirm qualitatively the validity of the numerical model. For reference, the area covering typical experimental conditions (i.e. $q_s/q_{ms} \sim 0.2/1.6 = 0.125$ and $k = 1 \times 10^{-9}$ to 4×10^{-9} cm^3 s^{-1} [40]) is shaded.

3.4. Experimental validation

3.4.1. Benchmarking of the optimized geometry

Fig. 7 compares the performance of the optimized LFSESI against a standard SESI. In both cases, for each sample flow rate, 23 fg/s of DEA were injected during 2 min. The injections were performed in triplicate for each sample flow rate investigated. The y-axis represents the integrated signal minus the baseline level, from the beginning of the injection until the signal level returns to the baseline. As predicted, the LFSESI ionization efficiency improves at decreasing sample flow rates. On the other hand, the standard non-optimized ionizer had an optimal performance around 0.9 L/min, dropping abruptly for lower sample flows, as expected. The improvement of the LFSESI over the standard SESI was a factor of five.

3.4.2. Detection of drugs

The analysis of vapor by SESI-MS has shown promise in a number of applications. We have recently shown that this technique could be used to investigate the in vivo pharmacokinetics of injected drugs in mice [42]. To further illustrate the capabilities of the optimized ionizer developed here, we tested its performance toward vapors of common drugs: melatonin, propofol, acetaminophen, pentobarbital and midazolam. Sample flow was set at an optimal value of 0.2 L/min. Fig. S2 displays the

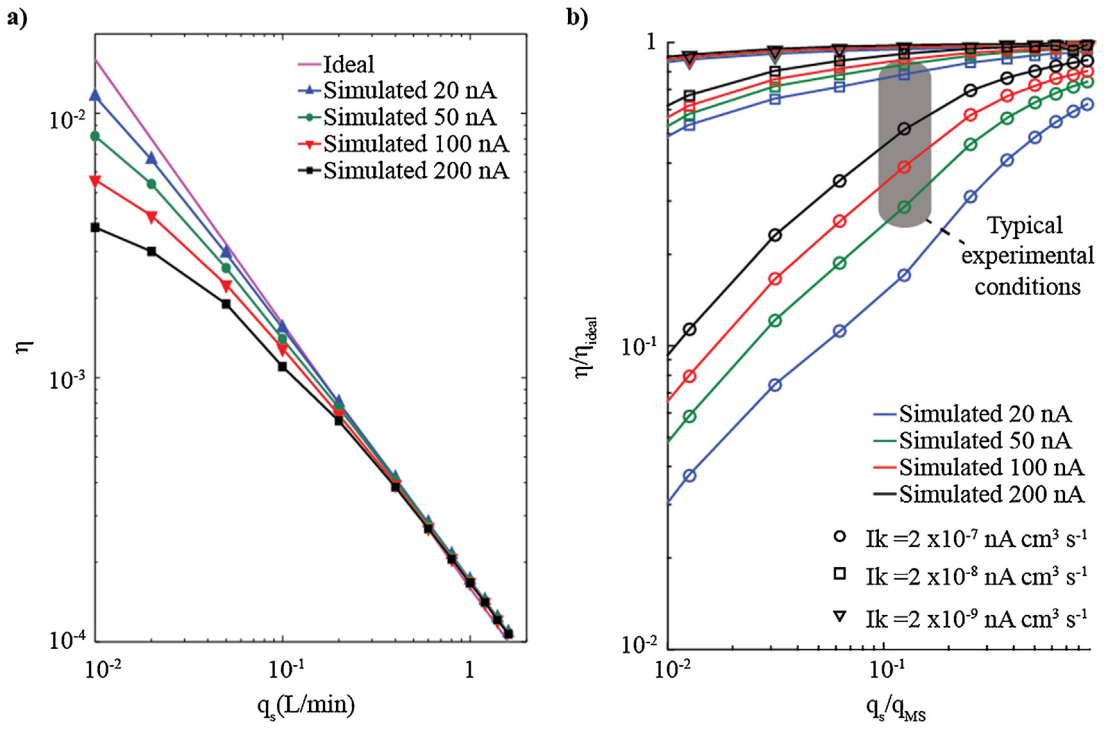

Fig. 6. (a) Ideal and simulated ionization efficiency for an electrospray H_2O-HCOOH (0.1%) and mass spectrometer sampling flow rate of 1.6 L/min at different electrospray currents. As expected, ionization efficiency increases with decreasing sample flow rate, but there exist a departure from the ideal behavior at flows below ~0.2 L/min; (b) ratio between simulated and ideal efficiencies vs. sample flow rate over MS flow rate for the combination of three different paired *Ik* values for four intensity values (20, 50, 100 and 200 nA). Note how the three *Ik* pairs tend to cluster together.

resulting mass spectra. The high resolution and mass accuracy of the Orbitrap mass spectrometer allows unambiguous detection of such drugs. Fig. 8 shows that the system was able to detect these drugs from concentrations of tenths of ppt in the gas phase, with a linear response across three orders of magnitude. Such low concentrations are deemed to be necessary to be detected in exhaled breath of small animals such as mice.

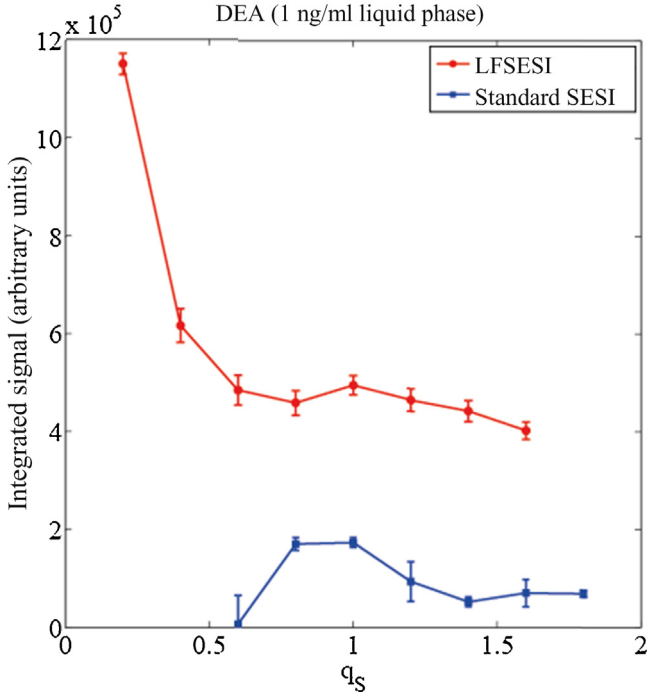

Fig. 7. Experimental performance of the optimized (LFSESI) and standard (SESI) ionizers; DEA 23 fg/s; electrospray of H_2O-HCOOH (0.1%).

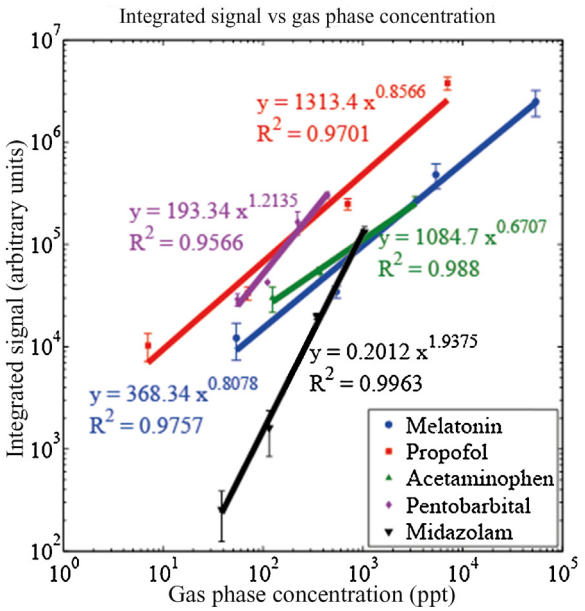

Fig. 8. Detection of several drugs ionized with the LFSESI developed in this work.

4. Conclusions

We have developed a complete numerical model for SESI, which is able to perform quantitative evaluation of this process. The key algorithm feature is a numeric electrospray model based purely on electrostatics, which gives reasonably accurate results at the required scale. The simplicity of this model allowed calculating the ionization of vapors by an electrospray cloud in a matter of minutes.

The analysis of the concentration distribution of species involved in SESI dynamics revealed that the common accepted

hypothesis of constant concentration of neutral vapors due the low Damköhler number ($p_i \sim 10^{-3}$–10^{-4}) is not valid when the sample flow is too low. In this situation, ionized vapors are driven too fast by electric fields to be replaced by new fresh neutral molecules, which result in a depletion of neutral vapors in the core of the ionization region. This effect causes ionization efficiency to be lower than the theoretically expected at very low sample flows.

Based on the numerical model, we constructed an optimized ionizer, which outperformed standard ionizers by a factor of 5 in terms of ionization efficiency. This add-on can be virtually interfaced with any commercial API-MS without any modification of the latter. As a result, pre-existing mass spectrometers can be deployed for the sensitive and real-time analysis of trace gases. We finally provided some examples on the detection of drugs, suggesting that such system can be suitable for real-time pharmacokinetic studies.

Acknowledgements

We gratefully acknowledge Dr. Juan Zhang (Novartis AG) for the donation of the LTQ Orbitrap instrument used in this study and the European Community's Seventh Framework Programme (FP7-2013-IAPP) for funding the project "Analytical Chemistry Instrumentation Development" (609691). We are indebted to Christoph Bärtschi (ETH workshop) for his assistance machining the ion source and Myriam Macía and Dr. Diego Gomez Garcia for assisting during the development phase. We are thankful to Prof. Juan Fernandez de la Mora (Yale) and Gonzalo Fernandez de la Mora (SEADM) for their continuous support of this project at all levels. We are thankful to Prof. Renato Zenobi for hosting us at ETH Zurich and for fruitful discussions.

Appendix A. Supplementary data

Supplementary data associated with this article can be found, in the online version, at http://dx.doi.org/10.1016/j.snb.2015.09.073.

References

[1] P. Kiselev, J.B. Fenn, ESIMS analysis of vapors at trace levels, in: Proceedings of the 49th ASMS Conference on Mass Spectrometry and Allied Topics, May 27–31, 2001, Chicago, IL, 2001.
[2] S. Fuerstenau, P. Kiselev, J.B. Fenn, ESIMS in the analysis of trace species in gases, in: Proceedings of the 47th ASMS Conference on Mass Spectrometry, Dallas, TX, 1999.
[3] S. Fuerstenau, Aggregation and Fragmentation in An Electrospray Ion Source, Yale University, New Haven, CT, 1994.
[4] C.M. Whitehouse, F. Levin, C.K. Meng, J.B. Fenn, Further adventures with an electrospray ion source, in: Proceedings of the 34th ASMS Conference, Cincinnati, OH, 1986.
[5] M. Yamashita, J.B. Fenn, Electrospray ion source: another variation on the free-jet theme, J. Phys. Chem. 88 (1984) 4451–4459.
[6] Y.H. Chen, H.H. Hill, D.P. Wittmer, Analytical merit of electrospray ion mobility spectrometry as a chromatographic detector, J. Microcolumn Sep. 6 (1994) 515–524.
[7] C.-Y. Lee, J. Shiea, Gas chromatography connected to multiple channel electrospray ionization mass spectrometry for the detection of volatile organic compounds, Anal. Chem. 70 (1998) 2757–2761.
[8] M. Tam, H.H. Hill, Secondary electrospray ionization-ion mobility spectrometry for explosive vapor detection, Anal. Chem. 76 (2004) 2741–2747.
[9] C. Wu, W.F. Siems, H.H. Hill, Secondary electrospray ionization ion mobility spectrometry/mass spectrometry of illicit drugs, Anal. Chem. 72 (2000) 396–403.
[10] W.E. Steiner, B.H. Clowers, P.E. Haigh, H.H. Hill, Secondary ionization of chemical warfare agent simulants: atmospheric pressure ion mobility time-of-flight mass spectrometry, Anal. Chem. 75 (2003) 6068–6076.
[11] M.Z. Huang, S.C. Cheng, Y.T. Cho, J. Shiea, Ambient ionization mass spectrometry: a tutorial, Anal. Chim. Acta 702 (2011) 1–15.
[12] T.R. Covey, B.A. Thomson, B.B. Schneider, Atmospheric pressure ion sources, Mass Spectrom. Rev. 28 (2009) 870–897.
[13] Z. Takáts, J.M. Wiseman, B. Gologan, R.G. Cooks, Mass spectrometry sampling under ambient conditions with desorption electrospray ionization, Science 306 (2004) 471–473.
[14] H. Chen, S. Yang, A. Wortmann, R. Zenobi, Neutral desorption sampling of living objects for rapid analysis by extractive electrospray ionization mass spectrometry, Angew. Chem. Int. Ed. 46 (2007) 7591–7594.
[15] B. Shrestha, A. Vertes, In situ metabolic profiling of single cells by laser ablation electrospray ionization mass spectrometry, Anal. Chem. 81 (2009) 8265–8271.
[16] D.-Y. Chang, C.-C. Lee, J. Shiea, Detecting large biomolecules from high-salt solutions by fused-droplet electrospray ionization mass spectrometry, Anal. Chem. 74 (2002) 2465–2469.
[17] P. Martínez-Lozano, J. Rus, G. Fernández de la Mora, M. Hernández, J. Fernández de la Mora, Secondary electrospray ionization (SESI) of ambient vapors for explosive detection at concentrations below parts per trillion, J. Am. Soc. Mass Spectrom. 20 (2009) 287–294.
[18] J.C. Wolf, M. Schaer, P. Siegenthaler, R. Zenobi, Direct quantification of chemical warfare agents and related compounds at low ppt levels: comparing active capillary dielectric barrier discharge plasma ionization and secondary electrospray ionization mass spectrometry, Anal. Chem. 87 (2015) 723–729.
[19] L. Meier, C. Berchtold, S. Schmid, R. Zenobi, High mass resolution breath analysis using secondary electrospray ionization mass spectrometry assisted by an ion funnel, J. Mass Spectrom. 47 (2012) 1571–1575.
[20] P. Martínez-Lozano, Mass spectrometric study of cutaneous volatiles by secondary electrospray ionization, Int. J. Mass Spectrom. 282 (2009) 128–132.
[21] P. Martínez-Lozano, J.F. de la Mora, Electrospray ionization of volatiles in breath, Int. J. Mass Spectrom. 265 (2007) 68–72.
[22] He J., P.M.L. Sinues, M. Hollmén, X. Li, M. Detmar, R. Zenobi, Fingerprinting breast cancer vs. normal mammary cells by mass spectrometric analysis of volatiles, Sci. Rep. 4 (2014).
[23] H.J. Martin, J.C. Reynolds, S. Riazanskaia, C.L.P. Thomas, High throughput volatile fatty acid skin metabolite profiling by thermal desorption secondary electrospray ionisation mass spectrometry, Analyst 139 (2014) 4279–4286.
[24] P. Martínez-Lozano Sinues, R.M. Alonso-Salces, L. Zingaro, A. Finiguerra, M.V. Holland, C. Guillou, et al., Mass spectrometry fingerprinting coupled to National Institute of Standards and Technology Mass Spectral search algorithm for pattern recognition, Anal. Chim. Acta 755 (2012) 28–36.
[25] H.D. Bean, T.R. Mellors, J. Zhu, J.E. Hill, Profiling aged artisanal Cheddar cheese using secondary electrospray ionization mass spectrometry, J. Agric. Food Chem. 63 (2015) 4386–4392.
[26] J. Zhu, H.D. Bean, J. Jiménez-Díaz, J.E. Hill, Secondary electrospray ionization-mass spectrometry (SESI-MS) breathprinting of multiple bacterial lung pathogens, a mouse model study, J. Appl. Physiol. (2013).
[27] J. Zhu, J. Jiménez-Díaz, H.D. Bean, N.A. Daphtary, M.I. Aliyeva, L.K.A. Lundblad, et al., Robust detection of *P. aeruginosa* and *S. aureus* acute lung infections by secondary electrospray ionization-mass spectrometry (SESI-MS) breathprinting: from initial infection to clearance, J. Breath Res. 7 (2013).
[28] N. Brenner, M. Haapala, K. Vuorensola, R. Kostiainen, Simple coupling of gas chromatography to electrospray ionization mass spectrometry, Anal. Chem. 80 (2008) 8334–8339.
[29] P. Martinez-Lozano Sinues, E. Criado, G. Vidal, Mechanistic study on the ionization of trace gases by an electrospray plume, Int. J. Mass Spectrom. 313 (2012) 21–29.
[30] J. Fernandez de la Mora, Ionization of vapor molecules by an electrospray cloud, Int. J. Mass Spectrom. 300 (2011) 182–193.
[31] G. Vidal-De-Miguel, A. Herrero, Secondary electrospray ionization of complex vapor mixtures: theoretical and experimental approach, J. Am. Soc. Mass Spectrom. 23 (2012) 1085–1096.
[32] G. Vidal-de-Miguel, M. Macía, P. Pinacho, J. Blanco, Low-sample flow secondary electrospray ionization: improving vapor ionization efficiency, Anal. Chem. 84 (2012) 8475–8479.
[33] A.M. Gañán-Calvo, J.C. Lasheras, J. Dávila, A. Barrero, The electrostatic spray emitted from an electrified conical meniscus, J. Aerosol Sci. 25 (1994) 1121–1142.
[34] J. Grifoll, J. Rosell-Llompart, Efficient Lagrangian simulation of electrospray droplets dynamics, J. Aerosol Sci. 47 (2012) 78–93.
[35] J. Fernandez de la Mora, The effect of charge emission from electrified liquid cones, J. Fluid Mech. 243 (1992) 561–574.
[36] P. Langevin, Une formule fondamentale de théorie cinétique, Ann. Chim. Phys. 5 (1905) 245–288.
[37] T. Su, M.T. Bowers, Ion-polar molecule collisions: the effect of ion size on ion-polar molecule rate constants; the parameterization of the average-dipole-orientation theory, Int. J. Mass Spectrom. Ion Phys. 12 (1973) 347–356.
[38] E.T.Y. Hsieh, A.W. Castleman Jr., A reconsideration of the theory of capture cross-sections for ion/molecule reactions and a total energy and angular momentum conserved average charge–dipole interaction theory (teams), Int. J. Mass Spectrom. Ion Phys. 40 (1981) 295–329.
[39] B.R. Eichelberger, T.P. Snow, V.M. Bierbaum, Collision rate constants for polarizable ions, J. Am. Soc. Mass Spectrom. 14 (2003) 501–505.
[40] J. Zhao, R.Y. Zhang, Proton transfer reaction rate constants between hydronium ion (H_3O^+) and volatile organic compounds, Atmos. Environ. 38 (2004) 2177–2185.
[41] P. Martínez-Lozano, L. Zingaro, A. Finiguerra, S. Cristoni, Secondary electrospray ionization-mass spectrometry: breath study on a control group, J. Breath Res. 5 (2011).
[42] X. Li, P. Martinez-Lozano Sinues, R. Dallmann, L. Bregy, M. Hollmén, S. Proulx, et al., Drug pharmacokinetics determined by real-time analysis of mouse breath, Angew. Chem. Int. Ed. (2015).

Biographies

César Barrios-Collado studied Industrial Engineering at the University of Valladolid (Spain). Since 2011, he has worked at SEADM S.L. on the development of a transversal modulation ion mobility spectrometer (TMIMS), with emphasis on the understanding of the ion optics within the TMIMS device. He is currently preparing his PhD dissertation at the University of Valladolid, under the supervision of Guillermo Vidal de Miguel. Throughout a collaborative project between SEADM and ETH-Zurich, he joined the group of Pablo Martinez-Lozano Sinues at the Laboratory of Organic Chemistry of ETH-Zurich in 2014. The main goal of this project is the development of pre-commercial instrumentation for vapor analysis.

Guillermo Vidal-de-Miguel studied Aeronautic Engineering at the Polytechnic University of Madrid and worked in EADS as an aerodynamicist and in Indra Systems on the optimization of Electronic Warfare Systems. In 2008 he joined the Mechanical Engineering group of Yale University for one year, and has led the R&D team at SEADM S.L. since 2009. During these years, he invented the low-flow secondary electropray ionization technology, and completed his PhD at the University of Valladolid. Currently, he is transferred to ETH-Zurich for a collaborative project between SEADM and ETH to develop instrumentation for analytical chemistry.

Pablo Martinez-Lozano Sinues graduated in Chemistry at the University of Murcia and earned his PhD in Mechanical Engineering at the University Carlos III of Madrid. He is currently completing his habilitation in Analytical Chemistry at the ETH-Zurich. He has been postdoctoral fellow at Yale University and the Italian National Research Council. In 2011 he was appointed senior scientist/lecturer at ETH Zurich within the group of Prof. R. Zenobi and since 2014 he is principal investigator. His research interests include the mass spectrometric analysis of trace gases for various interdisciplinary applications (e.g. diagnostic breath analysis).